JCI The Journal of Clinical Investigation

TLR9 signaling in fibroblastic reticular cells regulates peritoneal immunity

Li Xu, … , Timothy R. Billiar, Meihong Deng

J Clin Invest. 2019;129(9):3657-3669. https://doi.org/10.1172/JCI127542.

Research Article | Immunology | Inflammation

Graphical abstract

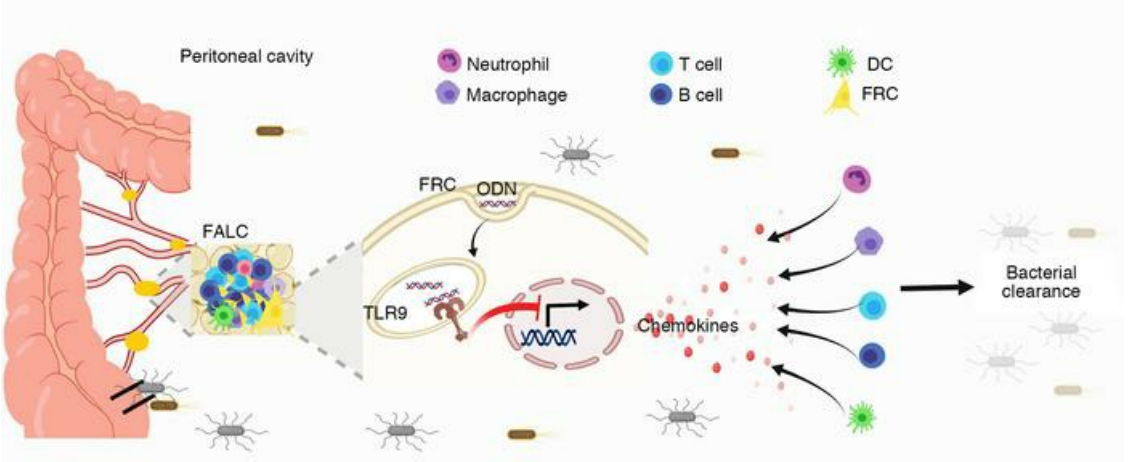

TLR9 signaling in fibroblastic reticular cells regulates peritoneal immunity

Li Xu,[1,2] Yiming Li,[1,3] Chenxuan Yang,[1,4] Patricia Loughran,[1,5] Hong Liao,[1] Rosemary Hoffman,[1] Timothy R. Billiar,[1] and Meihong Deng[1]

[1]Department of Surgery, University of Pittsburgh, Pittsburgh, Pennsylvania, USA. [2]Department of Emergency, Union Hospital, Tongji Medical College, Hua Zhong University of Science and Technology, Wuhan, China. [3]Department of Critical Care Medicine, Zhongnan Hospital of Wuhan University, Wuhan, China. [4]Tsinghua University School of Medicine, Beijing, China. [5]Center for Biologic Imaging, University of Pittsburgh, Pittsburgh, Pennsylvania, USA.

Fibroblastic reticular cells (FRCs), a subpopulation of stromal cells in lymphoid organs and fat-associated lymphoid clusters (FALCs) in adipose tissue, play immune-regulatory roles in the host response to infection and may be useful as a form of cell therapy in sepsis. Here, we found an unexpected major role of TLR9 in controlling peritoneal immune cell recruitment and FALC formation at baseline and after sepsis induced by cecal ligation and puncture (CLP). TLR9 regulated peritoneal immunity via suppression of chemokine production by FRCs. Adoptive transfer of TLR9-deficient FRCs more effectively decreased mortality, bacterial load, and systemic inflammation after CLP than WT FRCs. Importantly, we found that activation of TLR9 signaling suppressed chemokine production by human adipose tissue–derived FRCs. Together, our results indicate that TLR9 plays critical roles in regulating peritoneal immunity via suppression of chemokine production by FRCs. These data form a knowledge basis upon which to design new therapeutic strategies to improve the therapeutic efficacy of FRC-based treatments for sepsis and immune dysregulation diseases.

Introduction

Sepsis is now the leading cause of death in US hospitals and is projected to account for more than 5 million deaths globally each year (1–3). Currently, no effective treatments for sepsis are available. With an improved understanding of the overall disease process, scientists have developed single molecule–targeted therapies that modulate the activity of a specific pathway of the innate immune system, such as TLRs and proinflammatory cytokines. Clinical trials testing these agents have yielded little or no success, most likely due to the complex, multifaceted, and redundant nature of the host response to sepsis (4). Recently, this has led to a focus on cell-based therapies, founded on the notion that cells with immune-regulatory properties would improve outcomes in sepsis by influencing many different cells and molecular events (5, 6).

Fibroblastic reticular cells (FRCs), characterized as $CD45^-$, $CD31^-$, and $podoplanin^+$ ($PDPN^+$), are a unique subpopulation of stromal cells in lymphoid organs, such as lymph nodes and fat-associated lymphoid clusters (FALCs) (7, 8). FRCs are essential for the formation of lymphoid organs, as they fashion the scaffolding that recruits and supports immune cells (9–16). Besides their structural functions, FRCs have been recognized as major regulators of both innate and adaptive immunity in response to microbial pathogen invasion through interactions with neighboring immune cells within lymphoid tissues (9, 10, 14, 17). A single injection of ex vivo–expanded allogeneic lymph node–derived FRCs reduced mortality in cecal ligation and puncture–induced (CLP-induced) sepsis (17). FRCs are therefore attractive candidates for use as cell-based therapy in sepsis. A greater understanding of the cellular and molecular mechanisms of the effects of FRC in both health and disease may lead to more effective therapies employing modified FRCs.

Previous studies have shown that genetically and pharmacologically blocking TLR9 alleviates inflammation, organ damage, and mortality in mouse polymicrobial sepsis models (18–20). However, the mechanisms underlying the protective roles of TLR9 inhibition are unclear. A recent study in rodents demonstrated that FRCs in FALCs drive protective immunity in a myeloid differentiation primary response 88–dependent (MyD88-dependent) manner (14). TLR2 and TLR4 signaling via MyD88 play roles in the regulation of immunomodulatory functions of FRCs and enable them to orchestrate peritoneal immunity in mouse *Salmonella* infection (14). MyD88 is an important downstream adapter protein for many TLR- and cytokine-signaling pathways (e.g., TNF and IL-1) (21, 22). TLR9 is known to signal through MyD88 (21, 22); however, the role of TLR9 in regulating FRC function remains unknown.

In this study, we show that blocking TLR9 signaling increases peritoneal immune cell recruitment and FALC formation. TLR9 regulation of peritoneal immunity occurs via suppression of chemokine expression in FRCs. These findings not only address our knowledge gaps regarding the detrimental roles of TLR9 in sepsis, but also identify an unsuspected role for TLR9 in baseline FRC function and in peritoneal responses to bacterial infection. Modulating TLR9 signaling could improve the therapeutic efficacy of FRC-based sepsis therapies.

Results

TLR9 controls peritoneal immunity at baseline and during sepsis. We first confirmed the findings of others that genetically or pharma-

Authorship note: LX and YL are co–first authors. TRB and MD are co–senior authors.
Conflict of interest: The authors have declared that no conflict of interest exists.

Submitted: January 18, 2019; **Accepted:** June 4, 2019; **Published:** August 5, 2019.
Reference information: *J Clin Invest*. 2019;129(9):3657–3669.
https://doi.org/10.1172/JCI127542.

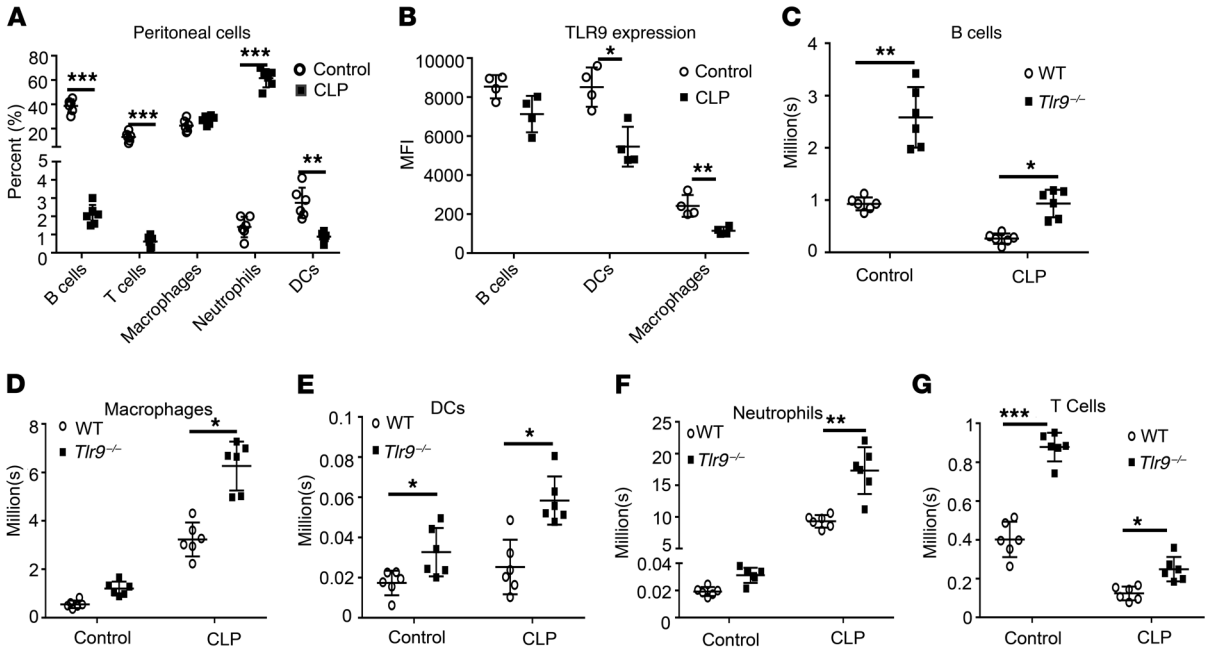

Figure 1. TLR9 controls peritoneal immunity at baseline and during sepsis. WT and *Tlr9*$^{-/-}$ mice were subjected to CLP. PLF was collected at 18 hours after CLP. (**A**) Percentages of indicated immune cells were measured by flow cytometry. (**B**) TLR9 expression in indicated peritoneal cells. MFI for TLR9 expression was measured by flow cytometry. (**C**–**G**) Peritoneal cell counts of (**C**) B cells, (**D**) macrophages, (**E**) DCs, (**F**) neutrophils, and (**G**) T cells in control and after CLP. Data are shown as mean ± SD from 2 separate experiments. Symbols represent individual mice. **P* < 0.05; ***P* < 0.01; ****P* < 0.001, unpaired, 2-tailed Student's *t* tests.

cologically blocking TLR9 reduces bacterial load, inflammation, and mortality in mouse polymicrobial sepsis (Figure 1, A–E; supplemental material available online with this article; https://doi.org/10.1172/JCI127542DS1; refs. 18–20). However, the mechanisms underlying the protection resulting from TLR9 suppression in sepsis are unclear. Recruitment of immune cells to infectious foci is an essential mechanism for peritoneal immunity and is critical for early bacterial clearance as well as prevention of an excessive inflammatory response (23, 24). Previous studies have reported that blocking TLR9 signaling increases immune cell recruitment into the peritoneal cavity after CLP (20). Here, we observed that total peritoneal cell counts were significantly higher in *Tlr9*$^{CpG1/CpG1}$ mutant mice and global *Tlr9*$^{-/-}$ mice compared with WT mice at baseline and after CLP (Supplemental Figure 1F). These data suggest that TLR9 may regulate host defense via modulation of peritoneal immunity. To understand the basis of TLR9 in the regulation of peritoneal immunity, we analyzed the cellular composition and TLR9 expression patterns in cells of the peritoneum. Peritoneal cell components were heterogenous at baseline and after CLP and included B cells, T cells, neutrophils, macrophages, and dendritic cells (DCs) (Figure 1A). At baseline, B cells were the dominant cell type, while neutrophils were recruited in large numbers after CLP and became the dominant cell type in the peritoneal cavity (Figure 1A). B cells, DCs, and macrophages expressed TLR9 (Figure 1B). However, the expression levels of TLR9 in DCs and macrophages significantly decreased after CLP compared with control levels (Figure 1B). The expression of TLR9 in T cells and neutrophils was undetectable by flow cytometry (Supplemental Figure 2). We next assessed the number of each cell type in peritoneal cavities of WT and *Tlr9*$^{-/-}$ mice using flow cytometry. Unexpectedly, numbers of all cell types were significantly higher in *Tlr9*$^{-/-}$ mice compared with WT mice before and after CLP (Figure 1, C–G). These data indicate that TLR9 controls the recruitment of not just one specific cell type, but all types of immune cells, into the peritoneal cavity at baseline and during sepsis.

B cells are required for the protective effects of Tlr9$^{-/-}$ *mice during sepsis*. The above data indicate that B cells are the dominant cell type in the peritoneal cavity at baseline. Furthermore, peritoneal B cells highly express TLR9 before and after CLP. B-1 cells, an innate-like B cell population, predominantly reside in body cavities and spontaneously secrete IgM as part of first-line host defenses against invading microorganisms (25–28). Consistent with the increased peritoneal B cell numbers in *Tlr9*$^{-/-}$ mice, peritoneal B-1 cell numbers and peritoneal IgM levels were significantly higher in *Tlr9*$^{-/-}$ mice compared with WT mice at baseline and after CLP (Figure 2, A–C). Upon activation, B-1 cells increase the production of cytokines such as GM-CSF to modulate macrophage and neutrophil functions (29). We observed that circulating and peritoneal GM-CSF levels were not detectable in control mice. However, peritoneal GM-CSF levels were significantly higher in *Tlr9*$^{-/-}$ mice compared with WT mice after CLP (Figure 2D). Circulating IgM and GM-CSF levels did not significantly differ between WT and *Tlr9*$^{-/-}$ mice at baseline or after CLP, suggesting that TLR9 had a local regulatory effect on peritoneal B-1 cells (Figure 2, B–D). To determine whether peritoneal B cells are required for the protective effects of TLR9 inhibition in sepsis, peritoneal B cells were depleted with CD19-neutralizing antibodies (Supplemental Figure 3). CD19-neutralizing antibodies significantly increased mortality and peritoneal bacterial load after

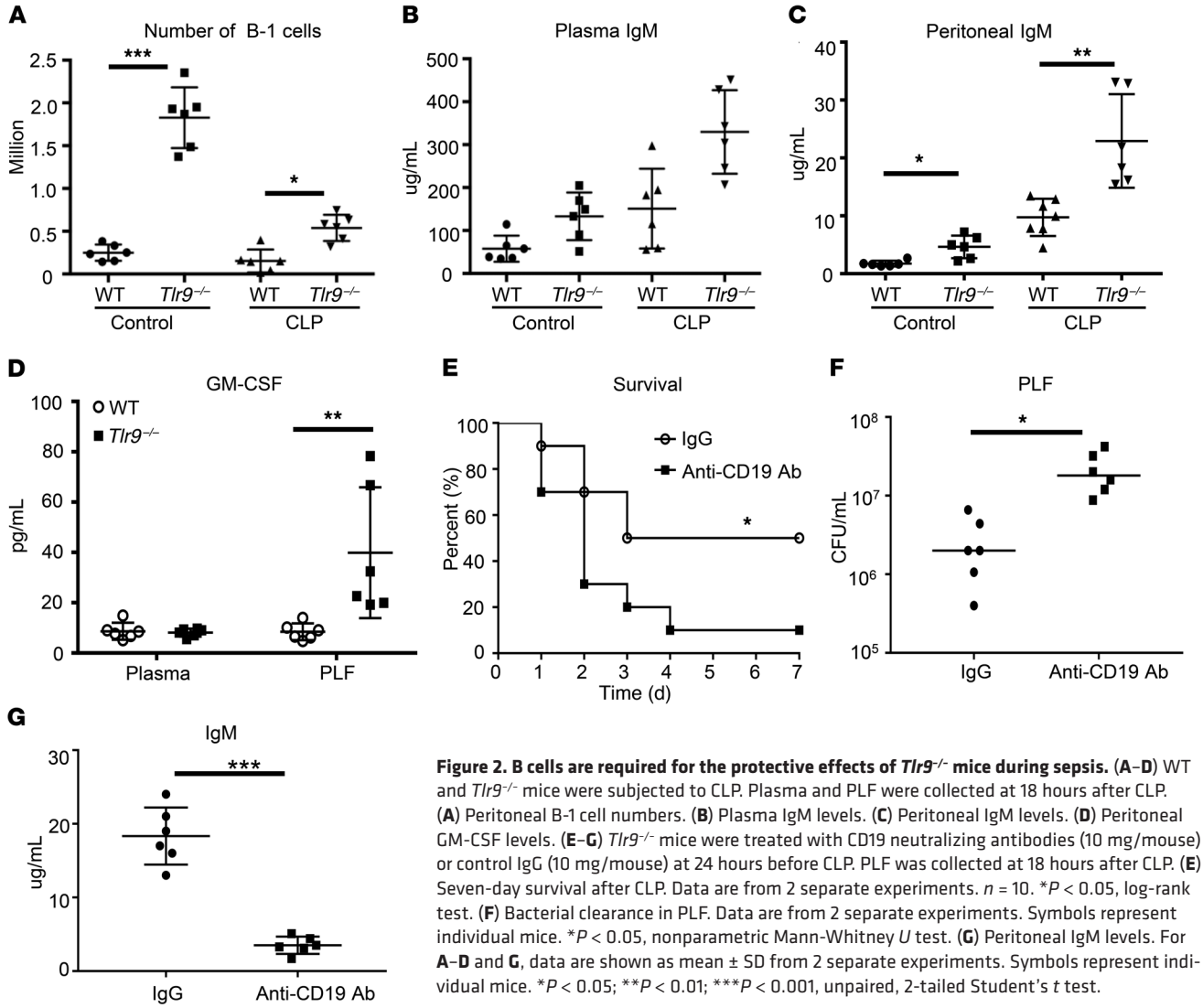

Figure 2. B cells are required for the protective effects of *Tlr9*$^{-/-}$ mice during sepsis. (**A**–**D**) WT and *Tlr9*$^{-/-}$ mice were subjected to CLP. Plasma and PLF were collected at 18 hours after CLP. (**A**) Peritoneal B-1 cell numbers. (**B**) Plasma IgM levels. (**C**) Peritoneal IgM levels. (**D**) Peritoneal GM-CSF levels. (**E**–**G**) *Tlr9*$^{-/-}$ mice were treated with CD19 neutralizing antibodies (10 mg/mouse) or control IgG (10 mg/mouse) at 24 hours before CLP. PLF was collected at 18 hours after CLP. (**E**) Seven-day survival after CLP. Data are from 2 separate experiments. $n = 10$. *$P < 0.05$, log-rank test. (**F**) Bacterial clearance in PLF. Data are from 2 separate experiments. Symbols represent individual mice. *$P < 0.05$, nonparametric Mann-Whitney U test. (**G**) Peritoneal IgM levels. For **A**–**D** and **G**, data are shown as mean ± SD from 2 separate experiments. Symbols represent individual mice. *$P < 0.05$; **$P < 0.01$; ***$P < 0.001$, unpaired, 2-tailed Student's t test.

CLP in *Tlr9*$^{-/-}$ mice compared with control IgG pretreatment (Figure 2, E and F). Peritoneal IgM levels were inversely correlated to bacterial load (Figure 2G). These results indicate that peritoneal B cells are required for the protective effects resulting from TLR9 deletion in sepsis.

TLR9 inhibits peritoneal B cell recruitment via suppressing CXCL13 production. We next tested whether TLR9 regulates B cell recruitment into the peritoneal cavity. CXCL13 is a selective B cell–attracting chemokine (30, 31). Notably, peritoneal CXCL13 levels in *Tlr9*$^{-/-}$ mice were significantly higher than in WT mice at baseline and after CLP (Figure 3A), suggesting that TLR9 may regulate peritoneal B cell recruitment via modulation of CXCL13 production. To determine whether CXCL13 is necessary for the protective effects of TLR9 in sepsis, WT and *Tlr9*$^{-/-}$ mice were treated with CXCL13-neutralizing antibodies and subjected to CLP. As expected, treatment with CXCL13-neutralizing antibodies significantly decreased peritoneal B-1 cell numbers and IgM levels in both WT and *Tlr9*$^{-/-}$ mice (Figure 3, B and C). Consistently, treatment with CXCL13-neutralizing antibodies also significantly impaired bacterial clearance and increased circulating IL-6 levels compared with control IgG treatment (Figure 3, D and E). Notably, treatment with CXCL13-neutralizing antibodies significantly increased mortality in *Tlr9*$^{-/-}$ mice compared with IgG treatment (Figure 3F). Furthermore, the addition of recombinant CXCL13 significantly increased peritoneal B-1 cell numbers and IgM levels in WT mice after CLP (Figure 3, G and H). Importantly, the addition of CXCL13 in WT mice significantly reduced bacterial load, circulating IL-6 levels, and mortality compared with PBS control treatment (Figure 3, I–K). These results indicate that TLR9 inhibits peritoneal B cell recruitment via the suppression of CXCL13 production during sepsis.

TLR9 in B cells does not account for the detrimental effects of TLR9 observed in sepsis. The above results indicate that B cells are required for the more efficient bacterial clearance observed in *Tlr9*$^{-/-}$ mice during sepsis. To determine whether TLR9 expressed by B cells is required for either B cell recruitment or function, we generated B cell–specific *Tlr9*$^{-/-}$ (*Cd19-Tlr9*$^{-/-}$) mice. Deletion of *Tlr9* in B cells was confirmed using flow cytometry (Supplemental Figure 4). There were no significant differences between *Cd19-Tlr9*$^{-/-}$ mice and the control *Tlr9*$^{loxp/loxp}$ (flox) mice in bacterial clearance, peritoneal total

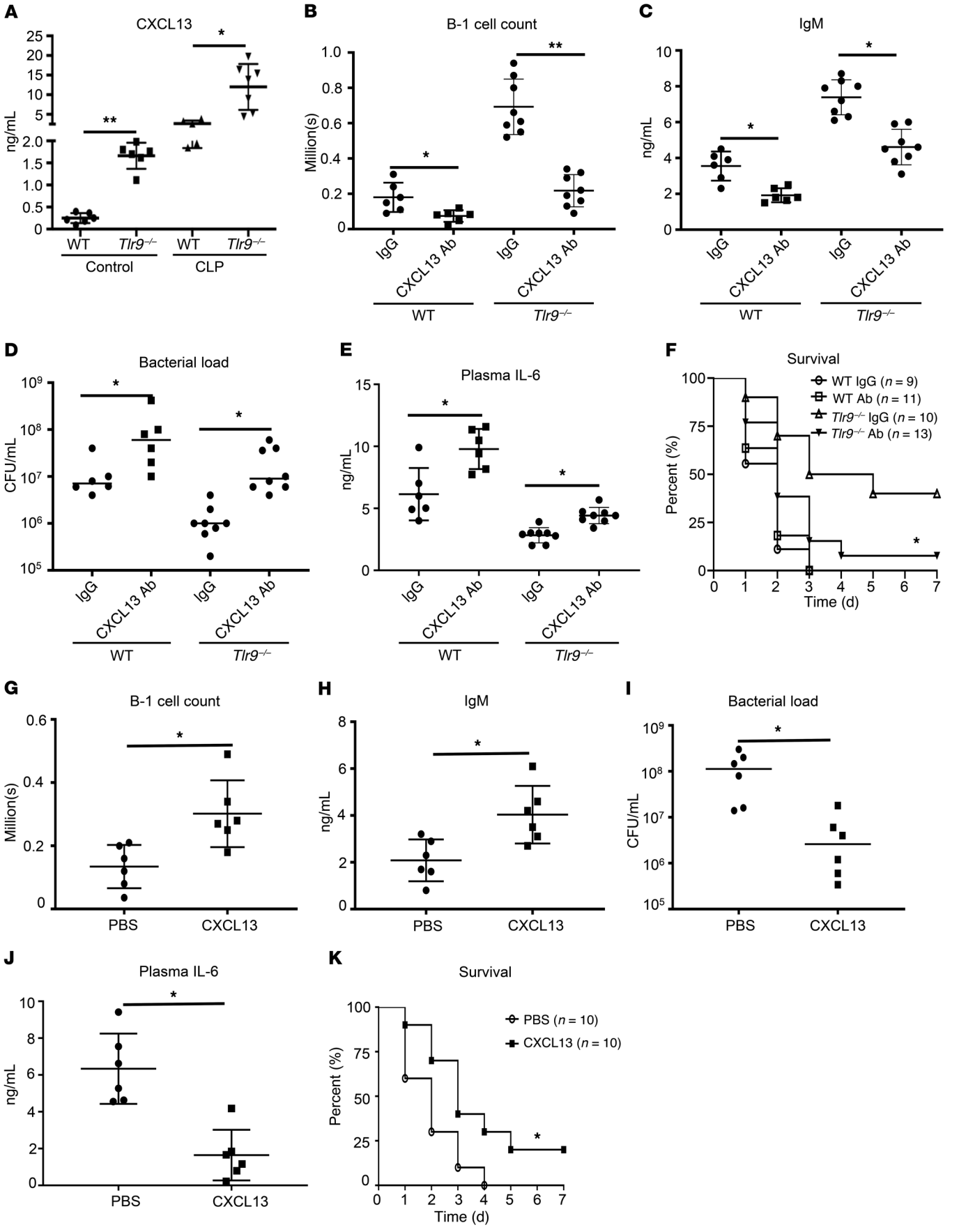
A
CXCL13
ng/mL
WT
Tlr9−/−
Control
CLP
B
B-1 cell count
Million(s)
IgG
CXCL13 Ab
C
IgM
D
Bacterial load
CFU/mL
E
Plasma IL-6
F
Survival
WT IgG (n = 9)
WT Ab (n = 11)
Tlr9−/− IgG (n = 10)
Tlr9−/− Ab (n = 13)
Percent (%)
Time (d)
G
H
I
J
K
PBS
CXCL13
PBS (n = 10)
CXCL13 (n = 10)

Figure 3. TLR9 inhibits peritoneal B cell recruitment via suppressing CXCL13 production. (**A**) WT and *Tlr9*$^{-/-}$ mice were subjected to CLP. PLF was collected at 18 hours after CLP. Peritoneal CXCL13 levels were assessed using ELISA. (**B**–**F**) WT and *Tlr9*$^{-/-}$ mice were treated with CXCL13 neutralizing antibodies (10 mg/mouse) or control IgG (10 mg/mouse) immediately after CLP. PLF and plasma were collected at 18 hours after CLP. (**B**) Peritoneal B-1 cell numbers. (**C**) Peritoneal IgM levels. (**D**) Bacterial load in PLF. (**E**) Plasma IL-6 levels. (**F**) Seven-day survival. For **A**–**C** and **E**, data are shown as mean ± SD. Symbols represent individual mice. *$P < 0.05$; **$P < 0.01$, unpaired, 2-tailed Student's *t* tests. For **D**, symbols represent individual mice. *$P < 0.05$, nonparametric Mann-Whitney *U* test. For **F**, $n = 13$–19/group as indicated. *$P < 0.05$ versus *Tlr9*$^{-/-}$ IgG, log-rank test. (**G**–**K**) WT mice were treated with recombinant CXCL13 (10 mg/mouse) or PBS immediately after CLP. (**G**) Peritoneal B-1 cell number. (**H**) Peritoneal IgM levels. (**I**) Bacterial load in PLF. (**J**) Plasma IL-6 levels. (**K**) Seven-day survival. For **G**, **H**, and **J**, data are shown as mean ± SD. Symbols represent individual mice. *$P < 0.05$, unpaired, 2-tailed Student's *t* test. For **I**, symbols represent individual mice. *$P < 0.05$, nonparametric Mann-Whitney *U* test. For **K**, $n = 10$/group. *$P < 0.05$, log-rank test.

cell count, B cell counts, and B-1 cell counts, or systemic and peritoneal IgM levels following CLP (Supplemental Figure 5, A–F). Importantly, *Tlr9* deletion in B cells did not affect CLP-induced increases in Cxcl13 production compared with WT mice (Supplemental Figure 5G). To further test the role of TLR9 in B-1 cell function, peritoneal B-1 cells were sorted from WT and *Tlr9*$^{-/-}$ mice and treated with or without a TLR9 agonist (ODN1585) and/or the TLR4 agonist LPS for 18 hours. We did not observe a significant difference in media IgM levels between WT and *Tlr9*$^{-/-}$ B-1 cell cultures (Supplemental Figure 5H), suggesting that TLR9 did not regulate IgM secretion from B-1 cells. Together, these data indicate that, while B-1 cells are required for the improved bacterial clearance observed in *Tlr9*-deficient mice, TLR9 in B cells does not contribute the antimicrobial functions of B-1 cells during peritoneal sepsis.

TLR9 inhibits CXCL13 expression in FRCs in mesenteric adipose tissues. The above results indicate that TLR9 inhibits peritoneal B cell recruitment via suppression of CXCL13 production; however, how TLR9 regulates peritoneal CXCL13 levels is unclear. CXCL13 is expressed in multiple cell types other than B cells (32), including DCs (33), macrophages (34), and FRCs in FALCs (9) and lymph nodes (35). We first tested to determine whether TLR9 regulated CXCL13 production from cells in the peritoneal cavity or cells from FALCs in mesenteric adipose tissues. Peritoneal cells and mesenteric adipose tissues were isolated from WT and *Tlr9*$^{-/-}$ mice before and after CLP. *Cxcl13* expression levels, assessed by PCR, in peritoneal cells did not significantly differ between WT and *Tlr9*$^{-/-}$ mice before or after CLP (Figure 4A). However, the expression of *Cxcl13* in mesenteric adipose tissues was significantly higher in *Tlr9*$^{-/-}$ mice than in WT mice before and after CLP (Figure 4B). These data suggest that TLR9 may regulate CXCL13 production from FALCs in mesenteric adipose tissues. To further identify the cell type in which TLR9 regulated CXCL13 production, mesenteric adipose tissues from WT and *Tlr9*$^{-/-}$ mice were isolated and subjected to immunofluorescence staining for CXCL13 as well as cell-specific markers (CD45 for hematopoietic cells including macrophages, T cells, B cells, and DCs; CD11c for DCs). CXCL13 rarely colocalized with CD45^{+} immune cells or CD11^{+} DCs (Figure 4C), suggesting that nonimmune cells in FALCs were a major source of CXCL13. FRCs, a subpopulation of stromal cells in FALCs, have been shown to express CXCL13 (9). To determine the role of TLR9 in the regulation of CXCL13 expression in FRCs, WT and *Tlr9*$^{-/-}$ FRCs were isolated from mesenteric adipose tissues and expanded ex vivo (Supplemental Figure 6). We found that FRCs constitutively expressed TLR9 (Supplemental Figure 6). Notably, *Cxcl13* expression was significantly downregulated in FRCs after stimulation with all 3 classes of TLR9 agonists (class A, ODN1585; class B, ODN1826; class C, ODN2395) compared with control (Figure 4D), while *Cxcl13* expression was not significantly downregulated after LPS (a TLR4 ligand) or Poly I:C (PIC) (a TLR3 ligand) stimulation (Figure 4D). Deletion of *Tlr9* in FRCs abrogated the suppressive effects of CpG1585 in *Cxcl13* expression (Figure 4E). These data reveal an unrecognized role of TLR9 in the regulation of FRC chemokine production.

TLR9 regulates peritoneal immunity via modulation of chemokine expression in FRCs. We next tested whether TLR9 also regulated chemokine expression in FRCs for the recruitment of other cell types in the peritoneal cavity. Cultured WT FRCs were stimulated with ODN1585, LPS, PIC, and ODN1585+LPS for 18 hours. The expression of chemokines in FRCs was assessed using quantitative PCR. Notably, activation of TLR9 signaling in FRCs with ODN1585 significantly reduced the expression of chemokines known to attract neutrophils (*Cxcl2* and *Cxcl5*), monocytes (*Cxcl3* and *Ccl2*), DCs (*Ccl19* and *Ccl2*), and lymphocytes (*Cxcl13*, *Ccl19*, and *Ccl21*) (Figure 5A). The expression of *Cxcl13*, *Cxcl3*, and *Ccl19* decreased dramatically after the addition of TLR9 agonists (Figure 5A). In contrast, stimulation with LPS increased the expression of *Cxcl13*, *Cxcl5*, *Cxcl2*, *Cxcl3*, *Ccl19*, and *Ccl2* in FRCs (Figure 5A), while stimulation with PIC increased the expression of *Cxcl2*, *Cxcl3*, *Ccl19*, *Ccl21* and *Ccl2* in FRCs (Figure 5A). These data suggest that individual TLRs play unique roles in regulating FRC responses to immune stimulators. Surprisingly, addition of ODN1585 suppressed LPS-induced *Cxcl5* expression in FRCs in a dose-dependent manner (Figure 5B). Furthermore, addition of ODN1585 suppressed the LPS-induced upregulation of *Cxcl13*, *Cxcl5*, *Cxcl2*, *Cxcl3*, and *Ccl2* expression in FRCs (Figure 5C). These data suggest a dominant role for TLR9 in FRCs that reside within the FALCs in the peritoneal cavity.

As FRCs have been shown to play essential roles in the formation of FALCs during the activation of host defenses, we next tested to determine whether TLR9 regulated FALC formation. Interestingly, the formation of FALCs as well as FALC total cell count in mesenteric adipose tissue was significantly higher in *Tlr9*$^{-/-}$ mice compared with WT mice at baseline and after CLP (Figure 5, D and E). It is known that B-1 cells migrate to FALC via CXCL13 during inflammation and thus are retained in the peritoneal cavity (9). Consistently, B-1 cell numbers in FALC increased significantly in both mouse strains after CLP compared with control (Figure 5F). Furthermore, B-1 cell numbers in FALC were significantly higher in *Tlr9*$^{-/-}$ mice compared with WT mice at baseline and after CLP (Figure 5F). These findings indicate that TLR9 plays critical roles in controlling peritoneal immunity and that the mechanisms are mediated via suppression of chemokine expression in FRCs for immune cell recruitment and FALC formation.

Blocking TLR9 signaling in FRCs increases the efficiency of FRC-based therapy for sepsis. A recent study showed that a single adoptive transfer of FRCs (10^6/mouse) improved survival after CLP (17). Our data indicate that TLR9 negatively regulates the

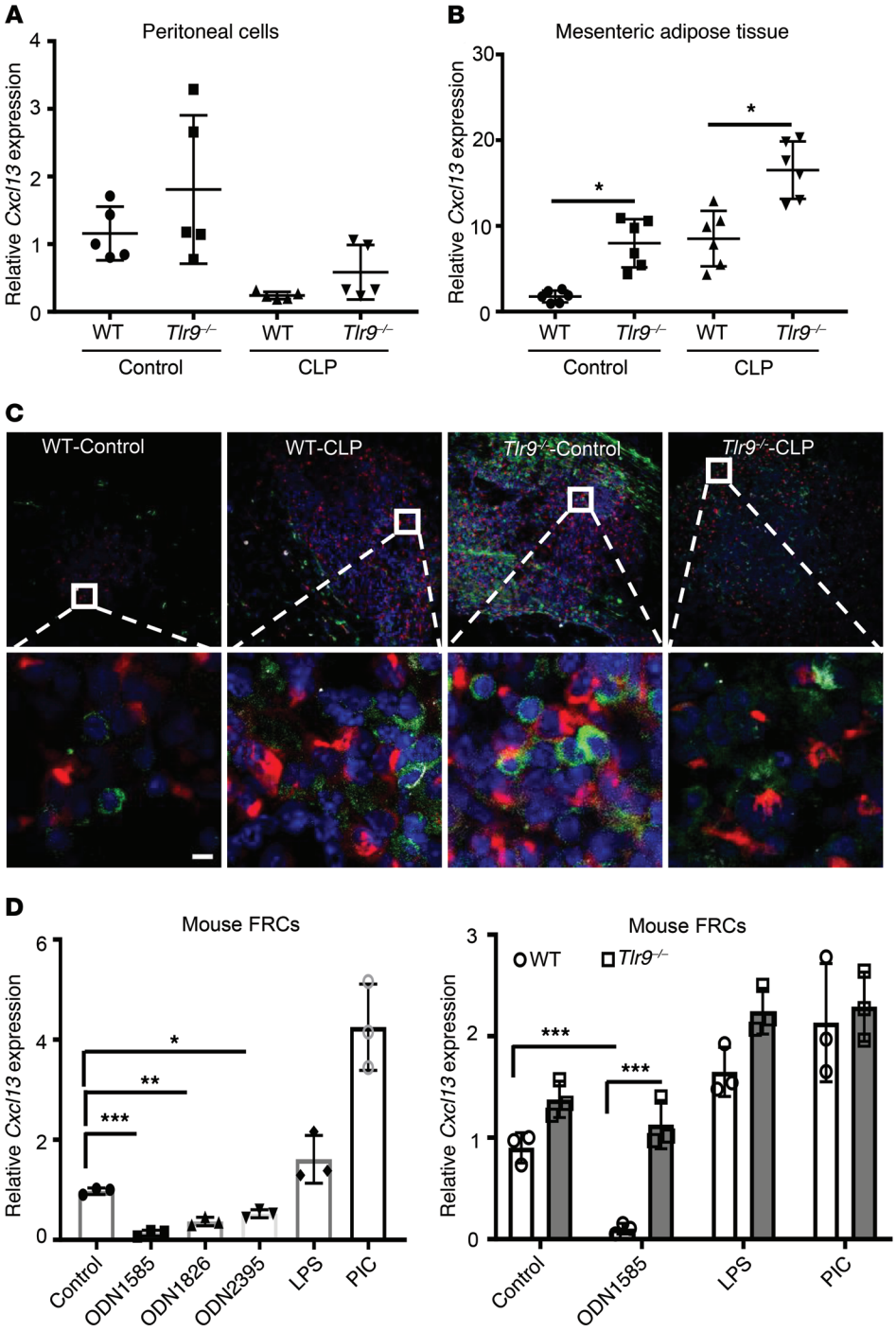

Figure 4. TLR9 inhibits CXCL13 expression in FRCs in mesenteric adipose tissues. (**A**–**C**) WT and *Tlr9*$^{-/-}$ mice were subjected to CLP. PLF and mesenteric adipose tissue were collected at18 hours after CLP. (**A** and **B**) Cxcl13 expression in peritoneal cells (**A**) and mesenteric adipose tissue (**B**) were assessed using quantitative PCR. Data are shown as mean ± SD from 2 separate experiments. Symbols represent individual mice. *$P < 0.05$, 2-tailed Student's *t* test. (**C**) Immunofluorescence staining of CXCL13 (red), CD45 (green), CD11c (white), and nucleus (blue) in mesenteric adipose tissue. Scale bar: 5 μm. (**D** and **E**) Cxcl13 expression in mouse FRCs. WT and *Tlr9*$^{-/-}$ FRCs were isolated from mesenteric adipose tissues and expanded ex vivo. FRCs were stimulated with indicated TLR ligands (ODN1585, 5 μM; ODN1826, 5 μM; ODN2395, 5 μM, LPS, 1 μg/mL; PIC, 20 μg/mL) for 18 hours. Cxcl13 expression was assessed using quantitative PCR. Data are shown as mean ± SD from 1 representative experiment. Experiments were performed 3 times. *$P < 0.05$; **$P < 0.01$; ***$P < 0.001$, 1-way ANOVA with Bonferroni's post hoc analysis.

establishment of peritoneal immunity via suppressing chemokine production in FRCs. Therefore, we hypothesized that blocking TLR9 signaling in FRCs may increase the efficiency of FRC-based therapy for sepsis. To test our hypothesis, WT mice were injected i.p. with WT or *Tlr9*$^{-/-}$ FRCs (2×10^5/ mouse) at an early time point (1 hour) or a late time point (12 hours) after CLP (Figure 6A). Adoptive transfer of this low number of WT FRCs at 1 hour after CLP only slightly reduced peritoneal bacterial load and IL-6 levels compared with PBS control (Figure 6, B and C). Furthermore, there was no significant difference in mortality between mice receiving adoptive transfer of WT FRCs and mice injected with PBS (Figure 6, D and E). Surprisingly, adoptive transfer of the same low number of *Tlr9*$^{-/-}$ FRCs at 1 hour after CLP significantly reduced peritoneal bacterial load and circulating IL-6 levels compared with PBS control (Figure 6, B and C). Notably, both early (1 hour after CLP) and late (12 hours after CLP) treatment with *Tlr9*$^{-/-}$ FRCs significantly reduced mortality compared with PBS control (Figure 6, D and E). These results support the idea that blocking TLR9 signaling in FRCs improves the efficiency of FRC-based therapy for sepsis.

TLR9 signaling suppresses chemokine production in human adipose tissue–derived FRCs. The above results indicate that TLR9 sig-

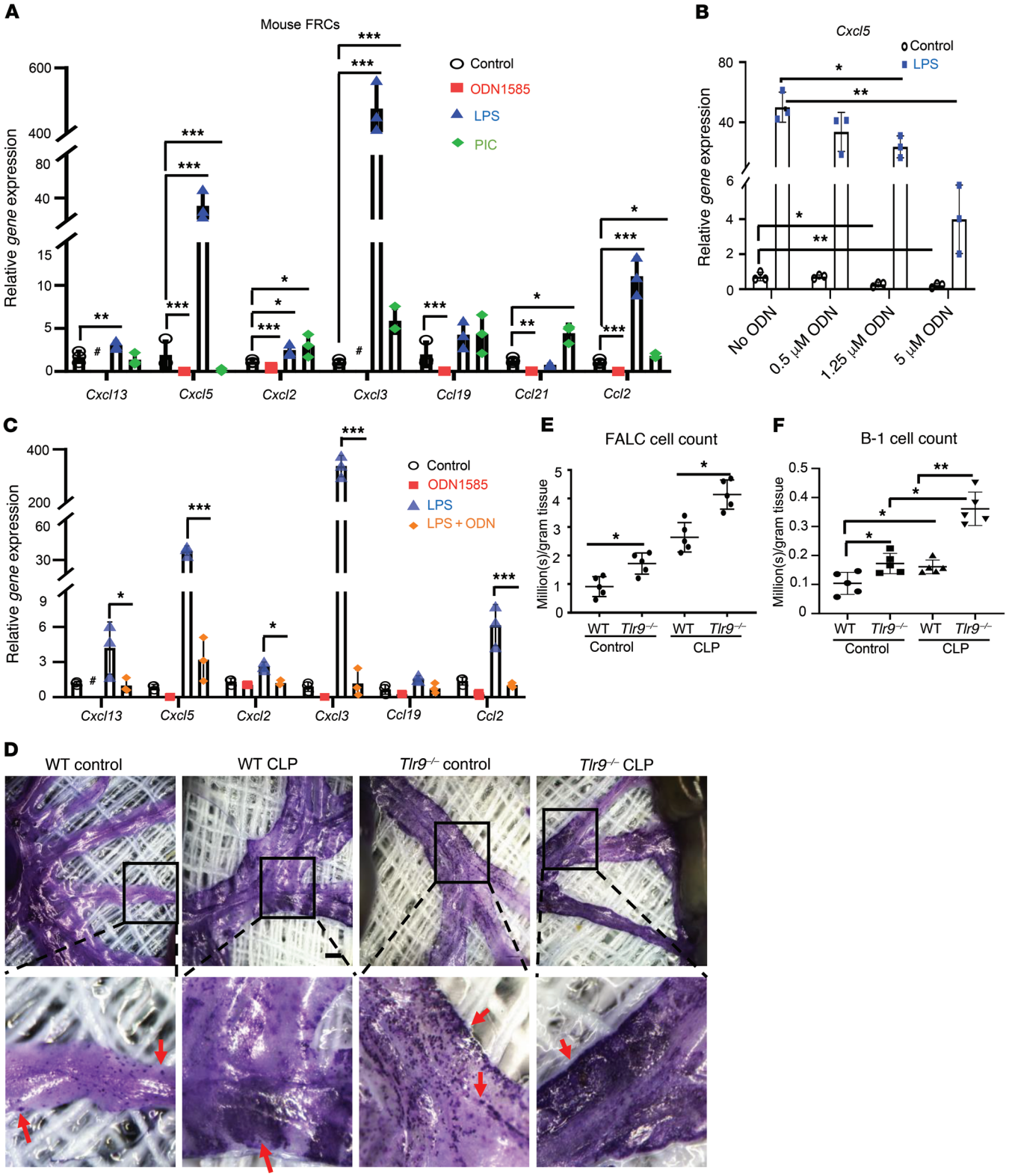

Figure 5. TLR9 regulates peritoneal immunity via modulation of chemokine expression in FRCs. (**A**–**C**) Chemokine expression in mouse FRCs. WT FRCs were isolated from mesenteric adipose tissues and expanded ex vivo. FRCs were stimulated with indicated TLR ligands (ODN: ODN1585, 5 μM; LPS, 1 μg/mL; PIC, 20 μg/mL; ODN+LPS: ODN1585, 5 μM +LPS, 1 μg/mL) for 18 hours. Indicated chemokine expression was assessed using quantitative PCR. Data are shown as mean ± SD from 1 representative experiment. Experiments were performed 3 times. *$P < 0.05$; **$P < 0.01$; ***$P < 0.001$, 1-way ANOVA with Bonferroni's post hoc analysis. #, not detectable. (**D**) FALCs in mesenteric adipose tissue were stained with 0.05% Toluidine Blue. Arrows indicate representative FALCs. Scale bar: 1 mm. (**E**) Total cell counts in mesenteric FALCs were measured using Cellometer. Data are shown as mean ± SD from 2 separate experiments. Symbols represent individual mice. *$P < 0.05$ vs. WT, 2-tailed Student's *t* test. (**F**) B-1 cell counts in mesenteric FALCs were measured using flow cytometry. Data are shown as mean ± SD from 2 separate experiments. Symbols represent individual mice. *$P < 0.05$, 1-way ANOVA with Bonferroni's post hoc analysis.

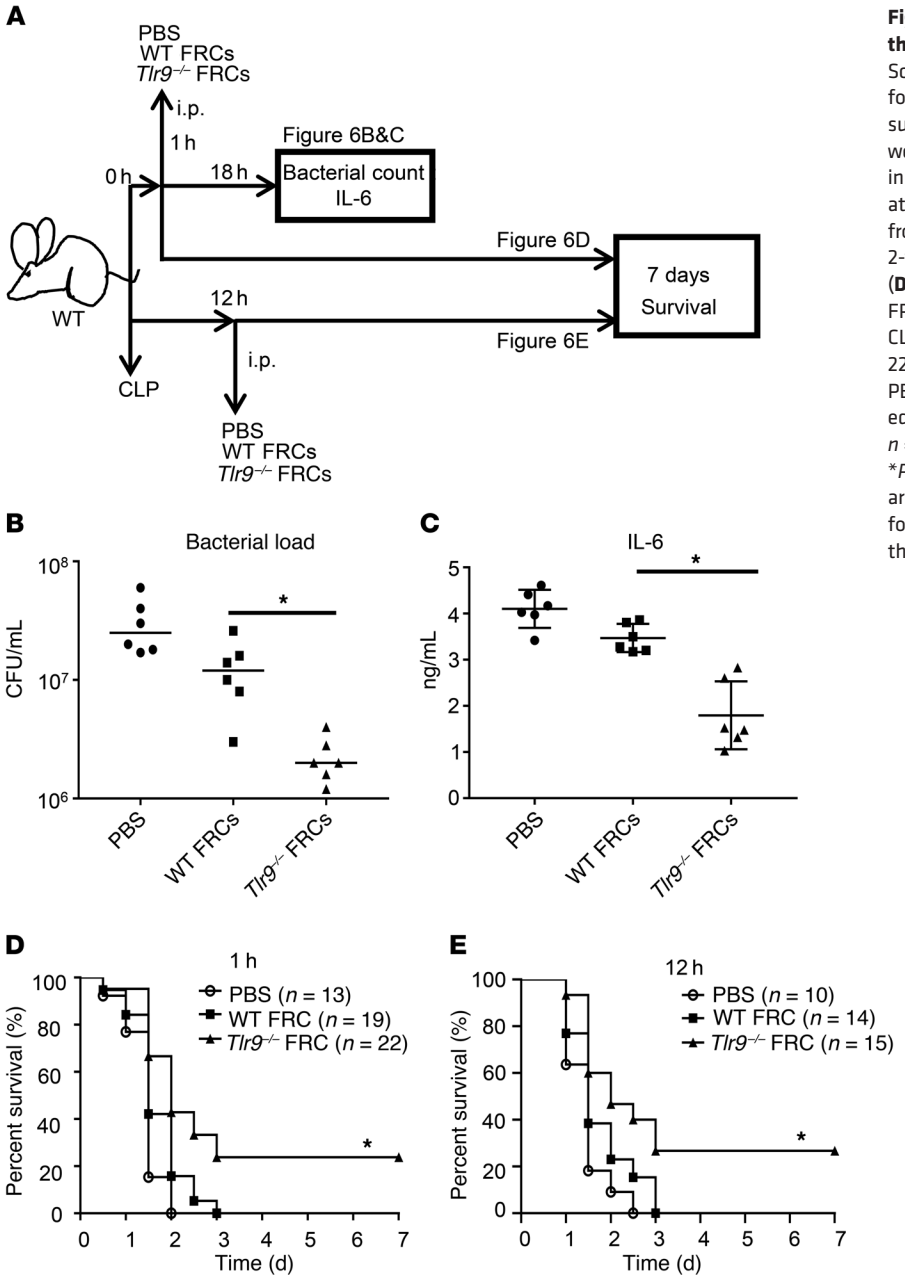

Figure 6. Blocking TLR9 signaling in FRCs increases the efficiency of FRC-based therapy for sepsis. (**A**) Schematic timeline of experimental set and analysis for adoptive transfer studies. (**B** and **C**) Mice were subjected to CLP. WT or *Tlr9*$^{-/-}$ FRCs (2×10^5/ mouse) were injected i.p. at 1 hour after CLP. (**B**) Bacterial load in PLF at 18 hours after CLP. (**C**) Circulating IL-6 levels at 18 hours after CLP. Data are shown as mean ± SD from 2 separate experiments. *$P < 0.05$, unpaired, 2-tailed Student's *t* test. (**D** and **E**) Seven-day survival. (**D**) Mice were subjected to CLP. PBS, WT, or *Tlr9*$^{-/-}$ FRCs (2×10^5/ mouse) were injected i.p. 1 hour after CLP. $n = 13$ in PBS group; $n = 19$ in WT FRC group; $n = 22$ in *Tlr9*$^{-/-}$ FRC group. (**E**) Mice were subjected to CLP. PBS, WT, or *Tlr9*$^{-/-}$ FRCs (2×10^5/ mouse) were injected i.p. at 12 hours after CLP. $n = 10$ in PBS group; $n = 14$ in WT FRC group; $n = 15$ in *Tlr9*$^{-/-}$ FRC group. *$P < 0.05$ vs. PBS, log-rank test. Data are from 3 separate experiments for **D** and 2 separate experiments for **E**. Statistical differences were determined using the log-rank test.

naling regulates peritoneal immunity via suppression of chemokine production in FRCs in a mouse model. To determine whether TLR9 signaling also regulates human FRC functions, we first tested whether FRCs are present in human adipose tissue. We successfully isolated FRCs from lipoaspirates human adipose tissue and expanded these ex vivo (Figure 7A). Human adipose tissue–derived FRCs also expressed TLR9 (Figure 7A). Importantly, we found that chemokine expression in human FRCs was significantly downregulated after class A TLR9 agonist (ODN2216) stimulation (Figure 7B). Therefore, our findings may provide a knowledge foundation for the FRC-based treatment of human sepsis.

Discussion

In studies aimed at understanding the detrimental roles of TLR9 in the host response to i.p. sepsis, we uncovered the finding that TLR9 plays critical roles in regulating peritoneal immunity via suppression of chemokine production in FRCs at baseline and during polymicrobial sepsis (Figure 8). Specifically, we discovered that FRCs constitutively express TLR9 and that activation of TLR9 signaling in FRCs suppresses the expression of chemokines, such as *Cxcl13*, *Ccl19*, *Ccl21*, *Cxcl2*, *Cxcl5*, *Cxcl3*, and *Ccl2*, which are essential for recruiting B cells, T cells, monocytes, and neutrophils into the peritoneal cavity as well as driving the formation of FALCs (Figure 8). The important regulatory role of TLR9 in FRCs was confirmed in FRCs derived from human adipose tissue. Furthermore, our data indicate that adoptive transfer of low numbers of *Tlr9*$^{-/-}$ FRCs protects mice from sepsis lethality. These findings unravel the mechanisms of protection against sepsis lethality previously observed with TLR9 inhibition and strongly suggest that DNA sensing through TLR9 by FRCs is an important regulatory

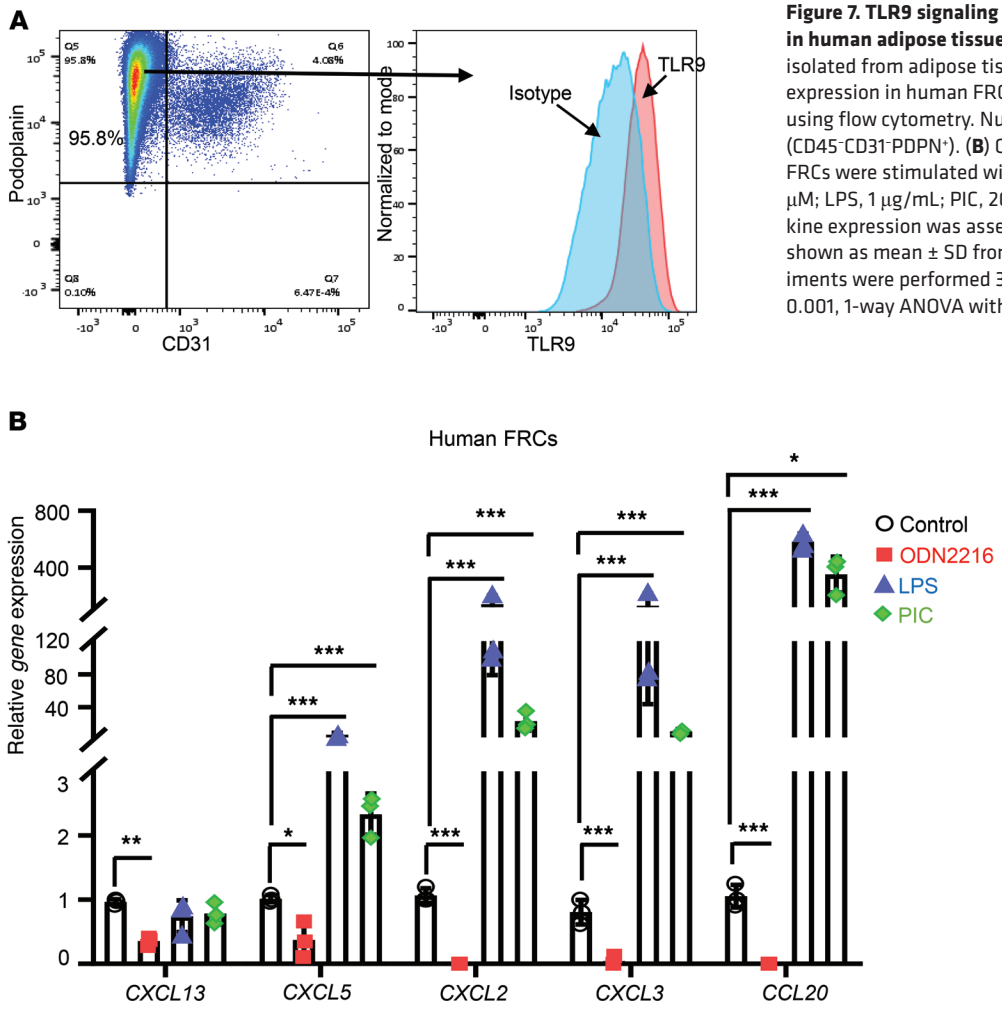

Figure 7. TLR9 signaling suppresses chemokine production in human adipose tissue–derived FRCs. Human FRCs were isolated from adipose tissue and expanded ex vivo. (**A**) TLR9 expression in human FRCs. TLR9 expression was assessed using flow cytometry. Numbers indicate percentage of FRCs ($CD45^-CD31^-PDPN^+$). (**B**) Chemokine expression in human FRCs. FRCs were stimulated with indicated TLR ligands (ODN2216, 5 μM; LPS, 1 μg/mL; PIC, 20 μg/mL) for 18 hours. Indicated chemokine expression was assessed using quantitative PCR. Data are shown as mean ± SD from 1 representative experiment. Experiments were performed 3 times. $^*P < 0.05$; $^{**}P < 0.01$; $^{***}P < 0.001$, 1-way ANOVA with Bonferroni's post hoc analysis.

step in controlling FALC formation and the trafficking of cells into the peritoneal cavity.

While it has been suspected that one possible mechanism underlying the detrimental roles of TLR9 in sepsis is impaired leukocyte recruitment into the peritoneal cavity (19, 20), we show here that deficiency of TLR9 generally increases the numbers of all peritoneal cell types, including B cells, T cells, neutrophils, macrophages, and DCs, as well as the formation of FALCs before and after CLP. Neutrophils are responsible for early bacterial clearance and, not surprisingly, have been shown to be necessary for the protective effects of TLR9 inhibition in CLP-induced sepsis (20). We show that peritoneal neutrophils express very low levels of TLR9 before and after CLP, which excludes the possibility that TLR9 in neutrophils directly regulates neutrophil function or recruitment. While B cells express abundant TLR9, deletion of *Tlr9* specifically in B cells did not mimic the effects of global *Tlr9* deletion at baseline or after CLP. DCs have been shown to produce chemokines that regulate neutrophil influx into tissues, including the peritoneum, and are known to express TLR9 (36). A previous study showed that deletion of TLR9 results in a higher number of peritoneal DCs after CLP (20). However, we found no role for TLR9 in the regulation of chemokine production by immune cells inside the peritoneal cavity and showed that DCs were not a major source of CXCL13 in FALC. In the setting of massive infections, as seen during the tissue necrosis and fecal contamination that occurs in the CLP model (as would be seen in gastrointestinal perforations in humans), it is likely that many pathogen-associated molecular patterns (PAMPs) are released, and these should activate other pattern recognition receptors that can drive immune responses in the peritoneum. For example, we have shown that TLR4 activation on DCs induces a robust IL-10 response (37). Our findings point to a dominant role for TLR9 in FRCs that reside with the FALCs in the peritoneal cavity. While TLR9 stimulation suppresses chemokine production by FRC, agonists that activate TLR3 or -4 enhanced chemokine production in these same cells. Notably, activation of the TLR9 signaling pathway markedly suppressed LPS-induced chemokine production by FRCs. Why TLR9 responses take priority within the FRC TLR signaling hierarchy at baseline and during CLP is not clear.

Peritoneal B cells, including B-1 cells, express abundant TLR9 and were the dominant cell type in the peritoneal cavity at baseline. B-1 cells are an innate-like B cell population predominantly residing in body cavities. These cells spontaneously produce most of the natural IgM antibodies required for pathogen opsonization and clearance (25–28). Our data indicate that peritoneal B cell and B-1 cell numbers, as well as associated peritoneal IgM levels, were markedly

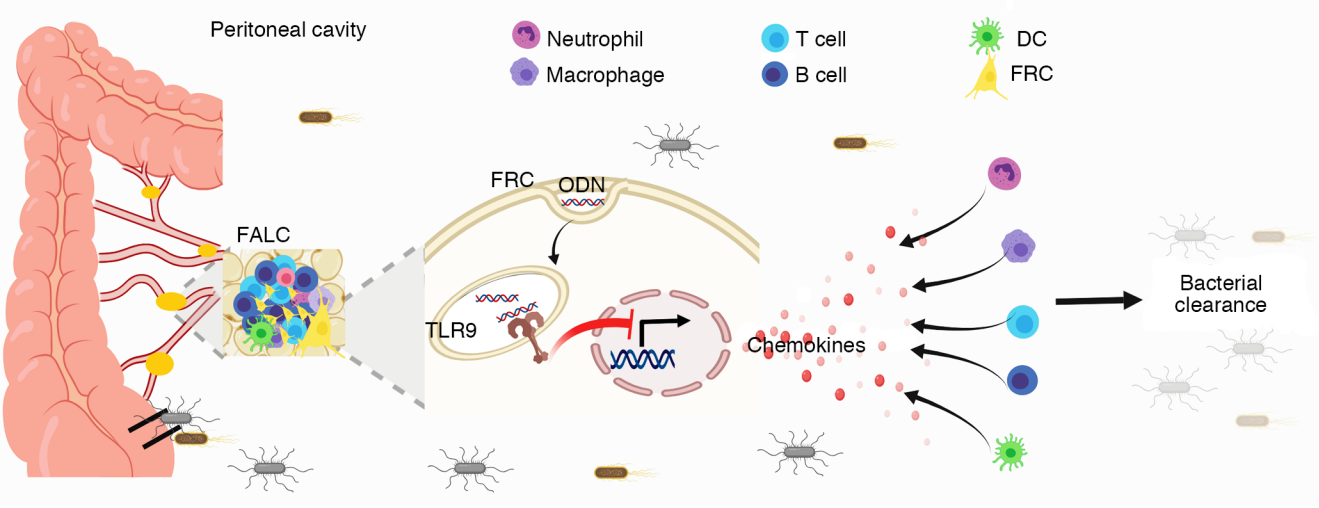

Figure 8. Schematic representation of TLR9 regulates peritoneal immunity via suppression of chemokine production by FRCs during polymicrobial sepsis. Activation of TLR9 signaling in FRCs suppresses the production of chemokines, which are essential for recruiting B cells, T cells, macrophages, and neutrophils into the peritoneal cavity as well as driving the formation of FALCs.

higher in *Tlr9*$^{-/-}$ mice compared with WT mice, and deletion of B cells reversed the protective effects of TLR9 deletion in CLP sepsis. The impact of TLR9 on B cell trafficking and B-1 cell function was not due to the activation of TLR9 in B cells, but instead mediated through the negative regulation of the critical B cell chemokine CXCL13 in FRCs. This was surprising considering the known roles of TLR9 in the regulation of B cell responses in other disease states, such as autoimmunity (38, 39), but here again, the CLP model results in the massive and acute release of many immune activators locally and systemically that may directly or indirectly regulate B cell responses. Although the numbers of peritoneal B-1 cells in *Tlr9*$^{-/-}$ mice decreased after CLP, peritoneal IgM levels markedly increased in *Tlr9*$^{-/-}$ mice after CLP compared with in controls. The decrease of B-1 cell numbers in the peritoneal cavity may be the result of B-1 cell migration to FALCs. B-1 cells are known to migrate to FALCs through CXCL13 and therefore are retained in the peritoneal cavity during inflammation (9). Consistent with this possibility, our data indicate CXCL13 expression in *Tlr9*$^{-/-}$ mesenteric adipose tissue was markedly higher compared with that in adipose tissue from WT mice after CLP. This was associated with enhanced FALC formation as well as markedly higher total cell numbers and B-1 cell numbers in FALC. The higher B-1 cell numbers in *Tlr9*$^{-/-}$ FALCs correlate with the higher levels of IgM in peritoneal cavities in *Tlr9*$^{-/-}$ mice compared with WT mice after CLP. The highly selective and major role for TLR9 on the FRCs in regulating the trafficking of peritoneal cells including B cells is surprising.

FRCs are a unique subpopulation of stromal cells that build the scaffolding for lymphoid organs, including lymph nodes and FALCs (7, 8, 13). Recently, FRCs have been recognized as major regulators of both innate and adaptive immunity in response to microbial pathogen invasion through interactions with neighboring immune cells within lymphoid tissues (9, 10, 14) as well as through the production of high levels of inflammatory cytokines and chemokines (7, 8). Mesenteric adipose tissue–derived FRCs have been shown to regulate inflammatory monocyte recruitment as well as the number of antibody-secreting B cells in the peritoneal cavity in a MyD88-dependent manner (14). TLR4 and TLR2 have been implicated in the regulation of immunomodulating functions of FRCs (14). However, the roles of individual TLR signaling in regulating FRC functions are unclear, and differential TLR/MyD88 signaling may have varying and even antagonistic effects (38–41). We observed marked increases in chemokine expression in FRCs after treatment with a TLR4 agonist, which can signal through MyD88 and Trif. Furthermore, we also found that stimulation with a TLR3 agonist (PIC), which signals through Trif, could increase chemokine expression in FRCs. However, activation of TLR9/MyD88 signaling with ODN1585 markedly suppressed chemokine expression in FRCs. The divergence of chemokine expression in response to TLR4 and TLR9 may be due to different signaling pathways downstream of MyD88. Furthermore, our data suggest that TLR9 signaling interacts with TLR4 signaling to control the chemokine production by FRCs. However, details on the TLR4 and TLR9 signaling pathways in FRCs require further study. The benefits to the host for TLR9 signaling to impair chemokine production through endosomal DNA sensing is unclear. However, the strong evidence that this inhibition takes place at baseline and in the absence of infections suggests that the role of TLR9 may be more important to suppressing chemokine production at baseline to prevent an overproduction of chemokines by the stroma in the resting state. The source of the DNA that drives this signaling is not revealed by our work, but could include dying cells or microbes.

Stromal cell–based therapy has been shown to have beneficial effects on various immune dysregulation diseases experimentally and clinically (6). However, the quantity of stromal cells required for therapeutic efficacy ranges from 2.5×10^5 cells/mouse to 40×10^6 cells/mouse in mouse sepsis models (6). The large numbers of stromal cells required for achieving therapeutic efficacy are not always available clinically. Therefore, new strategies are needed to improve the efficacy of stromal cell–based therapy. Lymph node–derived FRC transplant (1×10^6/mouse) reduced circulating

bacterial load and mortality in murine sepsis, which promises a possible FRC-based therapy for sepsis (17). However, the source of lymph node–derived FRCs is limited. Here we have shown that survival and bacterial clearance are improved in mice receiving adoptive transfer of relatively low numbers of *Tlr9*$^{-/-}$ FRCs (2×10^5 cells/mouse). Importantly, we identified FRCs in human adipose tissue from lipoaspirates. TLR9 also negatively regulates chemokine expression in human adipose tissue–derived FRCs. Large numbers of adipose FRCs can be easily obtained from lipoaspirates or during abdominal operations on healthy donors and rapidly expanded in vitro to generate a clinically effective number of FRCs. Therefore, adipose-derived FRCs are a potential source of cells for cell-based treatments.

In conclusion, we have provided compelling evidence showing that TLR9 plays critical roles in the regulation of peritoneal immunity for host defense. The mechanism underlying the regulation of TLR9 in peritoneal immunity occurs via suppression of chemokine expression in FRCs. These data address knowledge gaps on the mechanisms of TLR9 regulation of FRC pathobiology for host defense during sepsis. Finally, identification of human adipose tissue–derived FRCs and recognition of TLR9 in the regulation of chemokine expression in human FRCs provides a knowledge foundation for translating our findings into therapies for human sepsis.

Methods

Reagents. LPS-EK (LPS from *E. coli* K12), PIC low molecular weight (LMW), Mouse TLR9 Agonist Kit, and Human TLR9 Agonist Kit were purchased from InvivoGen. Mouse CXCL13/BLC/BCA-1 antibody, recombinant mouse CXCL13/BLC/BCA-1 protein, and normal goat IgG control were from R&D Systems. Anti-mouse CD19 neutralizing antibody (clone 1D3) and rat IgG2a isotype control (clone 2A3) were obtained from Bio X Cell.

Mice. WT C57BL/6 mice and *Cd19*$^{tm1(cre)Cgn/J}$ mice were purchased from the Jackson Laboratory. *Tlr9*$^{-/-}$ mice and *Tlr9*$^{loxp/loxp}$ (Flox) mice (42) on a C57BL/6 background were a gift from Mark J. Shlomchik (Department of Immunology, University of Pittsburgh). *Tlr9*$^{CpG1/CpG1}$ mutant mice (43) on a C57BL/6 background were a gift from Bruce Beutler (Center for the Genetics of Host Defense, UT Southwestern Medical Center, Dallas, Texas, USA). *Tlr9*$^{-/-}$ mice, *Tlr9*$^{fl/fl}$ mice, and *Tlr9*$^{CpG1/CpG1}$ mutant mice were bred in our animal facility. *Tlr9*$^{fl/fl}$ mice were interbred with heterozygous stud males to generate B cell–specific TLR9-deficient mice (*Tlr9*$^{loxP/Cd19-cre}$, *Cd19-Tlr9*$^{-/-}$). Transgenic mice used for experiments were confirmed to be the desired genotype via standard genotyping techniques. These animals were bred in our facility.

CLP procedure. Sepsis was induced by CLP. Both male and female mice that were 25 to 30 g in weight were used. The skin was disinfected with a 2% iodine tincture. Laparotomy was performed under 2% isoflurane (Piramal Critical Care) with oxygen. For the sublethal model, 50% of the cecum was ligated and punctured twice with a 22-gauge needle. Saline (1 mL) was given subcutaneously for resuscitation immediately after operation. Mice were sacrificed at 18 hours after CLP. For the lethal model, 75% of the cecum was ligated and punctured twice with an 18-gauge needle. Mice were monitored twice daily by personnel experienced in recognizing signs of a moribund state. Mice were euthanized with CO_2 when they became moribund or at observation end point (7 days). We used moribundity as the end point for our survival study following the Animal Research Advisory Committee Guidelines from NIH. *Isolation and ex vivo expansion of mouse FRCs*. Mesenteric adipose tissue was carefully excised from the small intestine, large intestine, and cecum using scissors without rupture of intestines and lymph nodes. Lymph nodes were removed. Adipose tissue was minced in digestion media (low glucose DMEM [Corning, Cellgro], 50 mM HEPES [Corning, Cellgro], 1% fatty acid free BSA [MilliporeSigma], Liberase TL [0.2 mg/mL, MilliporeSigma], DNase I [0.25 mg/mL, MilliporeSigma]) and agitated for 30 minutes at 37°C using magnetic stir bars and a multistirrer platform. Adipose tissue lysate was filtered through a 70 μM filter and spun down at 400 *g*. The pellet was resuspended in 100 μL of MACS buffer (Miltenyi Biotec). $CD45^+$ immune cells were depleted using mouse CD45 MicroBeads (Miltenyi Biotec) according to the manufacturer's instructions. The negatively isolated cells were centrifuged at 400 *g* for 5 minutes. The pellet was resuspended in MesenCult Expansion full media (STEMCELL Technology) and cultured at 37°C with 5% CO_2 for 7 days. The purity of FRCs ($CD45^-CD31^-PDPN^+$) was assessed using flow cytometry.

Culture of human FRCs. Human adipose tissue–derived stromal cells were obtained from the adipose stem cell center in the Department of Plastic Surgery at the University of Pittsburgh. Human adipose tissue–derived stromal cells were cultured and expanded in MesenCult Expansion full media (STEMCELL Technology) at 37°C with 5% CO_2 for 7 days. The purity of FRCs ($CD45^-CD31^-PDPN^+$) was assessed using flow cytometry.

Adoptive transfer of FRCs. Mesenteric adipose tissue-derived FRCs from WT or *Tlr9*$^{-/-}$ mice were generated in vitro as described above, and 2×10^5 FRCs were resuspended in PBS and injected i.p. into WT mice at 1 hour or 12 hours after CLP.

Bacterial culture. Peritoneal lavage fluid (PLF) and blood for bacterial culture were collected as mice were euthanized at 18 hours after CLP. PLF and blood were subjected to serial 10-fold dilutions and cultured at 37°C overnight in 5% sheep blood agar (Teknova). CFUs were quantified by manual counting.

Assessment of cytokine levels. Plasma and PLF samples were analyzed using IL-6, IL-1β, and CXCL13 ELISA kits from R&D Systems as well as an IgM ELISA kit from Invitrogen.

Immunofluorescence microscopy. For immunofluorescence staining of mesenteric adipose tissue, the whole animal was perfused with PBS and fixed in 2% paraformaldehyde. Tissue was then placed in 2% paraformaldehyde for 2 hours and then switched to 30% sucrose in distilled water solution for 12 hours. Whole-mount mesenteric adipose tissue was incubated with 2% BSA in PBS for 1 hour, followed by 5 washes with PBS containing 0.5% BSA (PBB). The samples were then incubated overnight with primary antibodies (rat anti-CD45 antibody, catalog 553076, BD Pharmingen; goat anti-CXCL13, catalog AF470, R&D Systems; hamster anti-CD11c, catalog MA11C5, BD Pharmingen). Samples were washed with PBS prior to incubation with secondary antibodies. Imaging conditions were maintained at identical settings within each antibody-labeling experiment, with original gating performed using the primary depletion control. Imaging was performed using a Nikon A1 confocal microscope. Quantification was performed using NIS Elements Software (Nikon).

Toluidine blue staining. Mesenteric adipose tissue was placed in 2% paraformaldehyde for 2 hours and then switched to 30% sucrose in distilled water solution for 12 hours. Whole-mount mesenteric adipose tissue was incubated with 0.1% Toluidine Blue (MilliporeSigma) in 1% sodium chloride (MilliporeSigma, pH 2.3) for 5 minutes, fol-

lowed by 10 washes with PBS. Mesenteric adipose tissue was imaged using an Olympus MVX10 Macroscope stand equipped with a Hamamatsu camera and an Olympus MV PLAPO 2XC objective. Data were acquired with NIS Elements (Nikon)

Flow cytometry. Cells were blocked for Fc receptors with anti-mouse CD16/32 (BD Bioscience) for 5 minutes and then were stained with fluorochrome-conjugated antibody (Supplemental Table 1) for 30 minutes, at 4°C in darkness. Data were acquired with a BD FACS LSR Fortessa Flow cytometer (BD Bioscience) and analyzed with FlowJo analytical software (TreeStar). Each experiment was repeated 3 times.

Comparative PCR analysis. Total RNA was extracted with the RNeasy Mini Extraction Kit (QIAGEN) according to the manufacturer's instructions. Two-step, real-time reverse transcription PCR (RT-PCR) was performed as previously described (44) with forward and reverse primer pairs prevalidated and specific for indicated target genes (Supplemental Table 2). All samples were assayed in duplicate and normalized to actin mRNA abundance.

Statistics. All data were analyzed using GraphPad Prism software (version 8.11). Unpaired, 2-tailed Student's *t* tests were used for comparisons between 2 groups. For multiple comparisons, 1-way ANOVA with Bonferroni's post hoc test was applied. For measurements of bacterial CFU, groups were compared using nonparametric Mann-Whitney *U* test. Survival data were analyzed using the log-rank test. A *P* value of less than 0.05 was considered statistically significant for all experiments. All values are presented as mean ± SD.

Study approval. All animal studies were approved by the Institutional Animal Care and Use Committees of the University of Pittsburgh.

Author contributions

MD and TRB conceived the project and wrote the manuscript. MD supervised the study, designed experiments, performed experiments, and analyzed the data. LX and YL performed experiments and analyzed the data. CY, PL, HL, and RH performed experiments. LX and YL contributed equally to this study. LX initiated this study and therefore is in the first position in the author list. MD and TB contributed equally to supervising this study. MD initiated and led this study and therefore is in the last position in the author list.

Acknowledgments

We thank Christine H. Burr for editing the manuscript. This work was supported by NIH grant R35-GM127027 (to TRB). Confocal microscopy performed at the University of Pittsburgh was made possible though NIH grant 1S10OD019973-01 (awarded to Simon C. Watkins).

Address correspondence to: Meihong Deng, Department of Surgery, University of Pittsburgh, NW607 MUH, 3459 Fifth Avenue, Pittsburgh, Pennsylvania 15213, USA. Phone: 412.647.6008; Email: dengm@upmc.edu.

1. Carney DE, Matsushima K, Frankel HL. Treatment of sepsis in the surgical intensive care unit. *Isr Med Assoc J*. 2011;13(11):694–699.
2. Daniels R. Surviving the first hours in sepsis: getting the basics right (an intensivist's perspective). *J Antimicrob Chemother*. 2011;66 Suppl 2:ii11–ii23.
3. Rudd KE, et al. The global burden of sepsis: barriers and potential solutions. *Crit Care*. 2018;22(1):232.
4. Vincent JL. Acute kidney injury, acute lung injury and septic shock: how does mortality compare? *Contrib Nephrol*. 2011;174:71–77.
5. Keane C, Jerkic M, Laffey JG. Stem Cell-based Therapies for Sepsis. *Anesthesiology*. 2017;127(6):1017–1034.
6. Laroye C, Gibot S, Reppel L, Bensoussan D. Concise Review: Mesenchymal Stromal/Stem Cells: A New Treatment for Sepsis and Septic Shock? *Stem Cells*. 2017;35(12):2331–2339.
7. Valencia J, et al. Characterization of human fibroblastic reticular cells as potential immunotherapeutic tools. *Cytotherapy*. 2017;19(5):640–653.
8. Malhotra D, et al. Transcriptional profiling of stroma from inflamed and resting lymph nodes defines immunological hallmarks. *Nat Immunol*. 2012;13(5):499–510.
9. Bénézech C, et al. Inflammation-induced formation of fat-associated lymphoid clusters. *Nat Immunol*. 2015;16(8):819–828.
10. Fletcher AL, et al. Lymph node fibroblastic reticular cells directly present peripheral tissue antigen under steady-state and inflammatory conditions. *J Exp Med*. 2010;207(4):689–697.
11. Cremasco V, et al. B cell homeostasis and follicle confines are governed by fibroblastic reticular cells. *Nat Immunol*. 2014;15(10):973–981.
12. Astarita JL, et al. The CLEC-2-podoplanin axis controls the contractility of fibroblastic reticular cells and lymph node microarchitecture. *Nat Immunol*. 2015;16(1):75–84.
13. Fletcher AL, Acton SE, Knoblich K. Lymph node fibroblastic reticular cells in health and disease. *Nat Rev Immunol*. 2015;15(6):350–361.
14. Perez-Shibayama C, et al. Fibroblastic reticular cells initiate immune responses in visceral adipose tissues and secure peritoneal immunity. *Sci Immunol*. 2018;3(26):eaar4539.
15. Brown FD, Turley SJ. Fibroblastic reticular cells: organization and regulation of the T lymphocyte life cycle. *J Immunol*. 2015;194(4):1389–1394.
16. Acton SE, et al. Dendritic cells control fibroblastic reticular network tension and lymph node expansion. *Nature*. 2014;514(7523):498–502.
17. Fletcher AL, et al. Lymph node fibroblastic reticular cell transplants show robust therapeutic efficacy in high-mortality murine sepsis. *Sci Transl Med*. 2014;6(249):249ra109.
18. Hu D, et al. Inhibition of Toll-like receptor 9 attenuates sepsis-induced mortality through suppressing excessive inflammatory response. *Cell Immunol*. 2015;295(2):92–98.
19. Tsuji N, Tsuji T, Ohashi N, Kato A, Fujigaki Y, Yasuda H. Role of mitochondrial DNA in septic AKI via Toll-like receptor 9. *J Am Soc Nephrol*. 2016;27(7):2009–2020.
20. Plitas G, Burt BM, Nguyen HM, Bamboat ZM, DeMatteo RP. Toll-like receptor 9 inhibition reduces mortality in polymicrobial sepsis. *J Exp Med*. 2008;205(6):1277–1283.
21. Balka KR, De Nardo D. Understanding early TLR signaling through the Myddosome. *J Leukoc Biol*. 2019;105(2):339–351.
22. Deguine J, Barton GM. MyD88: a central player in innate immune signaling. *F1000Prime Rep*. 2014;6:97.
23. Nathan C. Neutrophils and immunity: challenges and opportunities. *Nat Rev Immunol*. 2006;6(3):173–182.
24. Deng M, et al. Lipopolysaccharide clearance, bacterial clearance, and systemic inflammatory responses are regulated by cell type-specific functions of TLR4 during sepsis. *J Immunol*. 2013;190(10):5152–5160.
25. Baumgarth N, Herman OC, Jager GC, Brown LE, Herzenberg LA, Chen J. B-1 and B-2 cell-derived immunoglobulin M antibodies are nonredundant components of the protective response to influenza virus infection. *J Exp Med*. 2000;192(2):271–280.
26. Ochsenbein AF, et al. Control of early viral and bacterial distribution and disease by natural antibodies. *Science*. 1999;286(5447):2156–2159.
27. Haas KM, Poe JC, Steeber DA, Tedder TF. B-1a and B-1b cells exhibit distinct developmental requirements and have unique functional roles in innate and adaptive immunity to S. pneumoniae. *Immunity*. 2005;23(1):7–18.
28. Wang H, Coligan JE, Morse HC. Emerging functions of natural IgM and its Fc receptor FCMR in immune homeostasis. *Front Immunol*. 2016;7:99.
29. Cook AD, Braine EL, Hamilton JA. Stimulus-dependent requirement for granulocyte-macrophage colony-stimulating factor in inflammation. *J Immunol*. 2004;173(7):4643–4651.
30. Gunn MD, Ngo VN, Ansel KM, Ekland EH, Cyster JG, Williams LT. A B-cell-homing chemokine made in lymphoid follicles activates Burkitt's lymphoma receptor-1. *Nature*. 1998;391(6669):799–803.

31. Legler DF, Loetscher M, Roos RS, Clark-Lewis I, Baggiolini M, Moser B. B cell-attracting chemokine 1, a human CXC chemokine expressed in lymphoid tissues, selectively attracts B lymphocytes via BLR1/CXCR5. *J Exp Med*. 1998;187(4):655–660.
32. Litsiou E, et al. CXCL13 production in B cells via Toll-like receptor/lymphotoxin receptor signaling is involved in lymphoid neogenesis in chronic obstructive pulmonary disease. *Am J Respir Crit Care Med*. 2013;187(11):1194–1202.
33. Vissers JL, Hartgers FC, Lindhout E, Figdor CG, Adema GJ. BLC (CXCL13) is expressed by different dendritic cell subsets in vitro and in vivo. *Eur J Immunol*. 2001;31(5):1544–1549.
34. Bandow K, Kusuyama J, Shamoto M, Kakimoto K, Ohnishi T, Matsuguchi T. LPS-induced chemokine expression in both MyD88-dependent and -independent manners is regulated by Cot/Tpl2-ERK axis in macrophages. *FEBS Lett*. 2012;586(10):1540–1546.
35. Hähnlein JS, et al. Impaired lymph node stromal cell function during the earliest phases of rheumatoid arthritis. *Arthritis Res Ther*. 2018;20(1):35.
36. Guo Z, Zhang M, Tang H, Cao X. Fas signal links innate and adaptive immunity by promoting dendritic-cell secretion of CC and CXC chemokines. *Blood*. 2005;106(6):2033–2041.
37. Deng M, et al. Toll-like receptor 4 signaling on dendritic cells suppresses polymorphonuclear leukocyte CXCR2 expression and trafficking via interleukin 10 during intra-abdominal sepsis. *J Infect Dis*. 2016;213(8):1280–1288.
38. Christensen SR, Shupe J, Nickerson K, Kashgarian M, Flavell RA, Shlomchik MJ. Toll-like receptor 7 and TLR9 dictate autoantibody specificity and have opposing inflammatory and regulatory roles in a murine model of lupus. *Immunity*. 2006;25(3):417–428.
39. Nickerson KM, et al. TLR9 regulates TLR7- and MyD88-dependent autoantibody production and disease in a murine model of lupus. *J Immunol*. 2010;184(4):1840–1848.
40. Kfoury A, Virard F, Renno T, Coste I. Dual function of MyD88 in inflammation and oncogenesis: implications for therapeutic intervention. *Curr Opin Oncol*. 2014;26(1):86–91.
41. Salcedo R, Cataisson C, Hasan U, Yuspa SH, Trinchieri G. MyD88 and its divergent toll in carcinogenesis. *Trends Immunol*. 2013;34(8):379–389.
42. Garcia-Martinez I, et al. Hepatocyte mitochondrial DNA drives nonalcoholic steatohepatitis by activation of TLR9. *J Clin Invest*. 2016;126(3):859–864.
43. Tabeta K, et al. Toll-like receptors 9 and 3 as essential components of innate immune defense against mouse cytomegalovirus infection. *Proc Natl Acad Sci U S A*. 2004;101(10):3516–3521.
44. Deng M, Loughran PA, Zhang L, Scott MJ, Billiar TR. Shedding of the tumor necrosis factor (TNF) receptor from the surface of hepatocytes during sepsis limits inflammation through cGMP signaling. *Sci Signal*. 2015;8(361):ra11.